International Journal of Applied Engineering Research
ISSN 0973-4562 Volume 10, Number 11 (2015) pp. 30019-30028

http://www.ripublication.com

Numerical Investigation of Natural Convection Heat Transfer In A Square Cavity With The Influence of Prandtl Number

Chithra D[1], Eswaramurthi M.[2] and Sundararaj K[3].
[1]Assistant professor in Mathematics,
Amrita Vishwa Vidyapeetham, Coimbatore, India
[2] Professor in Mathematics, Amrita Vishwa Vidyapeetham, Erode, India
[3] Professor in Aeronautical Engineering,
Amrita Vishwa Vidyapeetham, Coimbatore, India
Correspondence to Chithra D., Department of Mathematics,
Amrita Vishwa Vidyapeetham, Vattamalaipalayam,
Coimbatore, Tamilnadu, India, Pincode:641 022
Email: devarajchithra@yahoo.co.in

Abstract

Natural convection heat transfer in enclosures find many applications such as heating and cooling of buildings, solar energy utilization, thermal energy storage, cooling of electrical and electronic components etc. In the present study, Numerical Investigation is conducted in a square cavity with one vertical wall maintained at a constant temperature and varying temperature in the opposing vertical wall. The governing vorticity and energy equations are solved by finite difference methods including Alternating Direction Implicit (ADI) and Successive Over Relaxation (SOR) techniques with C coding. Steady state isotherms and streamlines are obtained for Prandtl numbers 0.7(air) and 10.0(water). The contours of streamlines and isothermal lines are presented for all the range of temperatures investigated. Changes in the streamline and isothermal line patterns are observed with the change in Prandtl numbers and temperature values. The results obtained in this study are useful for the design of devices with enclosures subjected to temperature differences.

Keywords: Natural convection, ADI, SOR, Prandtl number, Grashof number.

Introduction

Natural convection heat transfer in enclosures has been extensively studied by researchers, because of its practical significance in science and technology. Applications include heating and cooling of buildings, solar energy collectors, heat exchangers and effective cooling of electronic components and machinery. The fluid flow and heat transfer behavior of such systems are analysed numerically and experimentally by a number of researchers with different boundary conditions.

An effective algorithm for the analysis of unsteady thermo capillary convection in a rectangular cavity was developed by Hamed and Folryan [1].Applying sudden heating along the free surface, by suddenly imposing known gas temperature variation across the cavity causes the unsteady liquid motion in the cavity with a passive gas over the surface. A coordinate transformation method is used to map the irregular computational domain and is then solved by the difference method. The field variables and unknown mapping functions are determined simultaneously using a picard- type iterative procedure. The algorithm is capable of very large time independent deformations of the liquid gas surface. Kazmierezak and Chinoda [2] investigated numerically the problem of laminar buoyancy driven flow of a fluid in a square cavity driven by a warm vertical wall having a uniform surface temperature whose magnitude is periodically changing. The effect of the periodically changing wall temperature is felt only partially into the enclosure and overall; the time-averaged heat transfer across the enclosure is rather insensitive to the time-dependent boundary condition. Schaldow et al [3] performed an additional run in which they ramped the driving wall temperature in a linear fashion over a five second interval equal in magnitude to the step change. Vasseur and Robillard [4] investigated the case of transient convective coding of a rectangular enclosure with end walls that continually decreased in temperature at a constant rate. Wilkes and Churchill [5] used an implicit-alternating direction finite difference method to study numerically the natural convection of a fluid contained in a long horizontal rectangular enclosure with vertical wall temperature for different Grashof number and aspect ratios. The natural convection in the presence of a magnetic field in a rectangular enclosure is studied by Rudhraiah et al [6] who established that the magnetic field dampens the rate of heat transfer and velocity profiles. Also the influence of magnetic field on the combined mechanism in a low Prandtl number fluid was studied. Kandaswamy et al [7] studied the natural convection heat transfer in a cavity with a variable viscosity fluid applying ADI method coupled with SOR technique in which the heat transfer rate is found to increase with an increase in viscosity of the fluid, where in they have chosen various Prandtl numbers like 0.05 (liquid metal), 0.7 (air) and 10 (water).

The objective of the present study is to numerically investigate in detail the natural convection in a two dimensional square cavity in which momentum transfer is significant. The details of geometry, numerical method applied and the results obtained are described in the following chapters.

Mathematical Formulation

A square cavity with different wall boundary conditions within which the fluid enclosed is considered for analysis. The geometry and temperature boundary conditions are shown in figure 1. Two of the opposing vertical walls are maintained at different temperatures. The horizontal walls are insulated from the surroundings.

When a fluid is enclosed within the cavity, it starts to circulate within the cavity and the heat transfers by natural convection from the hot wall to the cold wall.

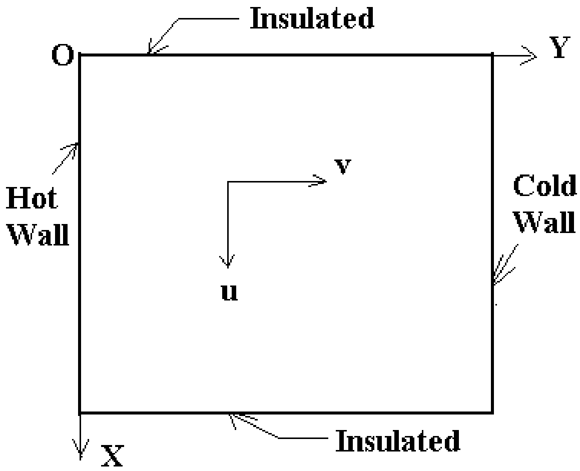

Figure 1: Schematic of the square enclosure

Governing Equations

The two-dimensional governing equations are

Continuity: $$\frac{\partial u}{\partial x}+\frac{\partial u}{\partial y}=0 \quad (1)$$

Momentum: $$\frac{\partial u}{\partial t}+u\frac{\partial u}{\partial x}+v\frac{\partial u}{\partial y}=-\frac{1}{\rho}\frac{\partial p}{\partial x}-g\beta(\theta-\theta_c)+\nu\nabla^2 u \quad (2)$$

$$\frac{\partial v}{\partial t}+u\frac{\partial v}{\partial x}+v\frac{\partial v}{\partial y}=-\frac{1}{\rho}\frac{\partial p}{\partial y}+\nu\nabla^2 v \quad (3)$$

Energy: $$\frac{\partial \theta}{\partial t}+u\frac{\partial \theta}{\partial x}+v\frac{\partial \theta}{\partial y}=\alpha\nabla^2\theta \quad (4)$$

Boundary Conditions

The initial and boundary conditions are,

$$t=0; \quad u=v=0,\ \theta=\theta_0,\ 0\le x\le L, 0\le y\le L$$

$$t>0; \quad u=v=0,\ \frac{\partial\theta}{\partial x}=0, \quad x=0$$

$$u=v=0,\ \frac{\partial\theta}{\partial x}=0, \quad x=L \quad (5)$$

$$u=v=0,\ \theta=\theta_h, \quad y=0$$

$$u=v=0,\ \theta=\theta_c, \quad y=L$$

Discretization of the governing equations

At any grid point, the term $\frac{\partial T}{\partial Y}$ in the energy equation, after nondimensionalising and the co-efficient velocities U & V are treated as constants over a time step. All space derivatives are given centered difference representations. The relevant finite-difference approximations to the energy equations, to be used consecutively over two half time steps, each of duration $\Delta\tau/2$ is,

For Y-direction,

$$T_{i,j-1}^{\ *}\left[\frac{-V_{i,j}^{\ n}}{2\Delta y}-\frac{1}{pr(\Delta y)^2}\right]+T_{i,j}^{\ *}\left[\frac{1}{\Delta\tau/2}+\frac{2}{pr(\Delta y)^2}\right]+T_{i,j+1}^{\ *}\left[\frac{V_{i,j}^{\ n}}{2\Delta y}-\frac{1}{pr(\Delta y)^2}\right]=$$
$$T_{i-1,j}^{\ n}\left[\frac{U_{i,j}^{\ n}}{2\Delta x}+\frac{1}{pr(\Delta x)^2}\right]+T_{i,j}^{\ n}\left[\frac{1}{\Delta\tau/2}-\frac{2}{pr(\Delta x)^2}\right]+T_{i+1,j}^{\ n}\left[\frac{-U_{i,j}^{\ n}}{2\Delta x}+\frac{1}{pr(\Delta x)^2}\right]$$

The above equation reduces to the tridiagonal form $AT_{i,j-1}^{\ *}+BT_{i,j}^{\ *}+CT_{i,j+1}^{\ *}=D$

where,

$$A=\left[\frac{-V_{i,j}^{\ n}}{2\Delta y}-\frac{1}{pr(\Delta y)^2}\right]$$

$$B=\left[\frac{2}{\Delta\tau}+\frac{2}{pr(\Delta y)^2}\right]$$

$$C=\left[\frac{V_{i,j}^{\ n}}{2\Delta y}-\frac{1}{pr(\Delta y)^2}\right]$$

$$D=T_{i-1,j}^{\ n}\left[\frac{U_{i,j}^{\ n}}{2\Delta x}+\frac{1}{pr(\Delta x)^2}\right]+T_{i,j}^{\ n}\left[\frac{2}{\Delta\tau}-\frac{2}{pr(\Delta x)^2}\right]+T_{i+1,j}^{\ n}\left[\frac{-U_{i,j}^{\ n}}{2\Delta x}+\frac{1}{pr(\Delta x)^2}\right]$$

For X-direction,

$$T_{i-1,j}^{\ n+1}\left[\frac{-U_{i,j}^{\ n}}{2\Delta x}-\frac{1}{pr(\Delta x)^2}\right]+T_{i,j}^{\ n+1}\left[\frac{1}{\Delta\tau/2}+\frac{2}{pr(\Delta x)^2}\right]+T_{i+1,j}^{\ n+1}\left[\frac{U_{i,j}^{\ n}}{2\Delta x}-\frac{1}{pr(\Delta x)^2}\right]=$$
$$T_{1,j-1}^{\ *}\left[\frac{V_{i,j}^{\ n}}{2\Delta y}+\frac{1}{pr(\Delta y)^2}\right]+T_{i,j}^{\ *}\left[\frac{1}{\Delta\tau/2}-\frac{2}{pr(\Delta y)^2}\right]+T_{i,j+1}^{\ *}\left[\frac{-V_{i,j}^{\ n}}{2\Delta y}+\frac{1}{pr(\Delta y)^2}\right]$$

The above equation reduces to the tridiagonal form:

$$AT_{i-1,j}^{\ n+1}+BT_{i,j}^{\ n+1}+CT_{i+1,j}^{\ n+1}=D$$

where,

$$A = \left[\frac{-U_{i,j}{}^{n}}{2\Delta x} - \frac{1}{pr(\Delta x)^2}\right]$$

$$B = \left[\frac{2}{\Delta\tau} + \frac{2}{pr(\Delta x)^2}\right]$$

$$C = \left[\frac{U_{i,j}{}^{n}}{2\Delta x} - \frac{1}{pr(\Delta x)^2}\right]$$

$$D = T_{1,j-1}{}^{*}\left[\frac{V_{i,j}{}^{n}}{2\Delta y} + \frac{1}{pr(\Delta y)^2}\right] + T_{i,j}{}^{*}\left[\frac{2}{\Delta\tau} - \frac{2}{pr(\Delta y)^2}\right] + T_{i,j+1}{}^{*}\left[\frac{-V_{i,j}{}^{n}}{2\Delta y} + \frac{1}{pr(\Delta y)^2}\right]$$

Similar approximations also hold for the vorticity equation which precedes the stream function across a time step.

Method of Solution

The governing equations- energy, vorticity and stream function are solved via a finite difference technique consisting of Alternating Direction Implicit (ADI) and Successive Over Relaxation (SOR) methods. The added advantage of using this unconditionally stable numerical scheme is that larger time increments may be used without loss of stability. The vorticity and temperature equations are parabolic, while the stream function equation is elliptic. The resulting stream function values are then used to determine the velocity components and the boundary values of the vorticity. Thus the sequence beginning with the solution of the energy equation is applied repeatedly until the desired results are obtained. The convergence criterion used for the field variables ϕ is

$$\frac{\phi_{n+1}(i,j) - \phi_n(i,j)}{\phi_{n+1}(i,j)} \le 10^{-5}$$

In the above expression the subscript n refers to appropriate time level and ϕ represents T, ς $and \psi$. The mesh 51 x 51 was opted as the ideal one with a suitable time increment. In this study a computational code, using ‘C’ language is developed to obtain the finite difference solution implementing Alternating Direct Implicit (ADI) and Successive Over Relaxation (SOR) methods. On execution the code generates the data file containing all the flow field variables such as temperature, velocity components, stream functions and vorticity. The contour plots for various quantities are plotted using MATLAB.

Results and Discussion

In the present study, numerical experiments were conducted for two different fluids of Prandtl numbers 0.7 (air) and 10.0 (water). The specified initial and boundary conditions were imposed and for all the cases analyzed the maximum temperature at the hot wall is T_{max} =2.0 and the temperature at the cold wall T_{min} is varied from 2.0 to -6.0. Using streamline plots the direction of fluid velocity at various points in the cavity and also the regions of high and low velocities could be found for different Prandtl numbers. Using isothermal plots the regions of high and low temperature gradient could be found. Since the boundary temperatures and Prandtl number influence the distribution of momentum and temperature significantly within the cavity, different patterns of streamline and isotherms were obtained. For all the cases analyzed, steady state isothermal and streamlines are obtained for a standard Grashof number 20000.

Natural convection with Prandtl number 0.7

Figure 2 shows the contour plots of streamlines and isotherms for different boundary temperatures. As the Prandtl number is less than one, the thermal diffusivity is more predominant than the momentum diffusivity within the cavity region. Due to this, the streamline patterns in all the figures are similar whereas significant changes are observed in isotherms. The streamlines in Figure 2 with T_{max} = 2 and T_{min} = 2, show that the fluid circulates within the cavity along the streamline. Low stream line spacing close to the bottom wall indicate higher fluid velocities in comparison with the low velocities associated with the coarse spacing near the top wall. The unsymmetrical nature of the streamline pattern is due to thermal gradient which exists only along Y direction and buoyancy force which acts only along X direction. The temperature gradients are observed along the Y direction and comparatively high temperature gradients could be noticed near the right boundary. In the region close to the left boundary the fluid particles move in the upward direction and deflected downward by the upper boundary. Streamlines close to the region near the top right boundary show the existence of the circulatory flow. Subsequently, as the temperature of the right boundary decreases up to T_{min} = - 6.0, this recirculation zone disappears and the streamline pattern becomes symmetrical about the vertical axis passing through the centre of the cavity. As the boundary temperature difference is increased, the gradient increases at all the points within the cavity.

Natural convection with Prandtl number 10.0

When the Prandtl number is greater than one, the momentum diffusivity is more predominant than the thermal diffusivity within the cavity region. Figure 3 shows the streamlines and isotherms for different boundary temperatures with Prandtl number 10.0. Significant changes in streamline formation could be observed as the temperature difference between the left and right boundary is increased. As the temperature difference decreases the recirculatory zone vanishes and the magnitude of the vertical component of velocity increases. Increase in velocity close to the right boundary could be observed as the streamline spacing decreases. The direction of vertical component of velocity is upward close to the left boundary for all the test conditions. The changes in streamline pattern with raise in temperature difference shows that the magnitude of vertical component of velocity initially increases and then decreases gradually. There is a recirculatory flow created in the region near the centre of the cavity which increases in size with the increase in temperature difference. Streamline patterns plotted also show that the recirculation zone created at the centre of the cavity moves towards the right boundary. Since the Pr >>1, the changes in temperature distribution within the cavity is comparatively low. For all the cases analyzed the temperature gradient are found to exist near the left and right boundary. Over a larger region at the centre of the cavity uniform temperature could be observed.

Conclusion

A finite difference technique is applied using ‘C’ language to predict the natural convection heat transfer in an enclosed cavity consisting of a fluid, with different wall boundary temperatures. The numerical results are obtained for two different Prandtl numbers (0.7 and 10.0) of fluid. The influences of wall boundary temperature and Prandtl number of fluid within the cavity on flow pattern and temperature distribution are analyzed in detail. The results obtained are presented in the form of contours of streamlines and isotherms using MATLAB. Significant changes in distribution of temperature within the cavity could be observed when the Prandtl number is less than unity. The results obtained with Prandtl number more than one, show considerable changes in streamline pattern inducing vortices within the cavity. This study will be useful in the design of devices consisting of fluid with different wall boundary temperature.

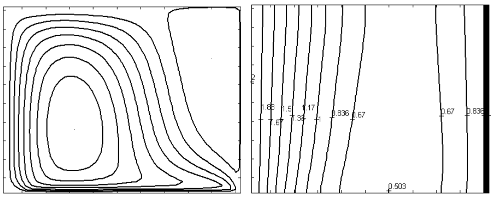

T_{min} = 2.0; T_{max} = 2.0

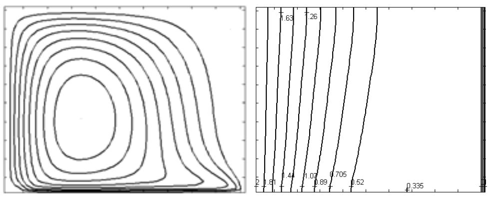

T_{min} = 1.0; T_{max} = 2.0

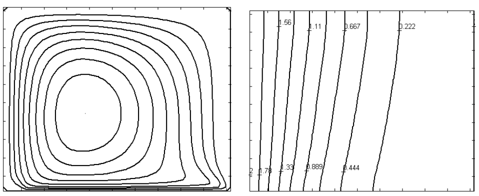

T_{min} = 0.0; T_{max} = 2.0

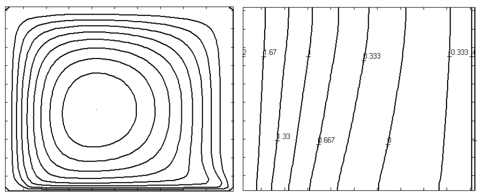

T_{min} = -1.0 ; T_{max} = 2.0

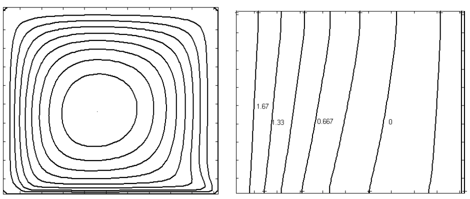

T_{min} = -2.0; Tmax = 2.0

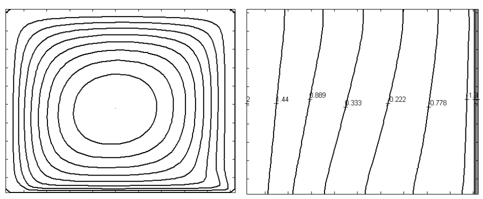

T_{min} = -3.0; T_{max} = 2.0

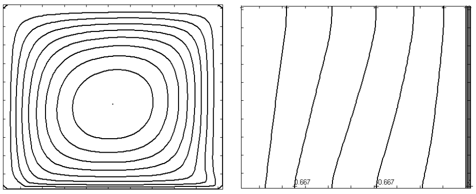

T_{min} = -4.0; T_{max} = 2.0

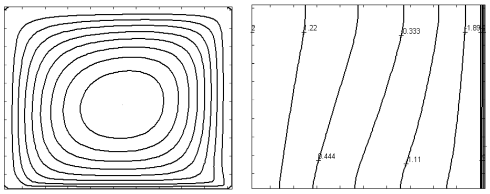

Tmin = -5.0; Tmax = 2.0

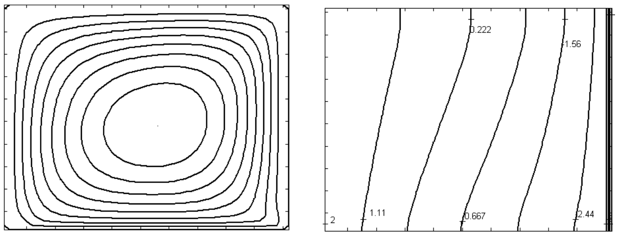

T_{min} = -6.0 and T_{max} = 2.0

Figure 2: Steady state streamlines and isotherms for Pr = 0.7

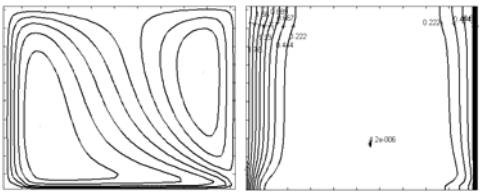

T_{min} = 2.0;T_{max} = 2.0

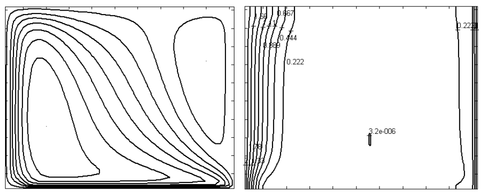

T_{min} = 1.0; T_{max} = 2.0

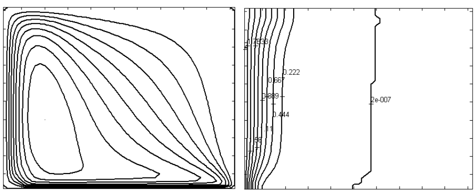

T_{min} = 0.0; T_{max} = 2.0

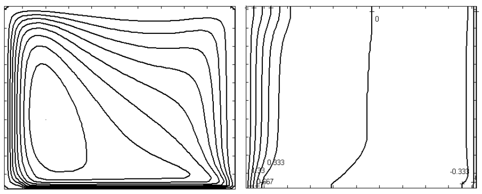

T_{min} = -1.0; T_{max} = 2.0

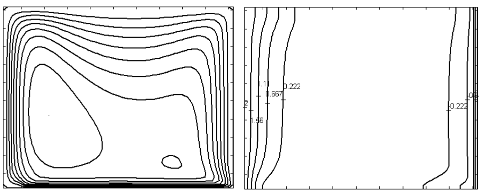

T_{min} = -2.0 and T_{max} = 2.0

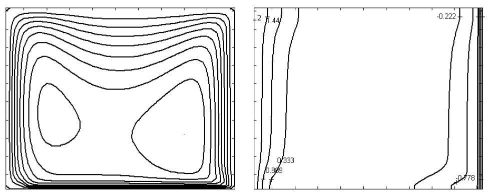

T_{min} = -3.0 and T_{max} = 2.0

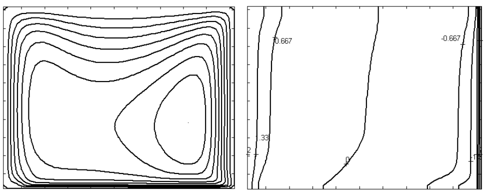

T_{min} = -4.0 and T_{max} = 2.0

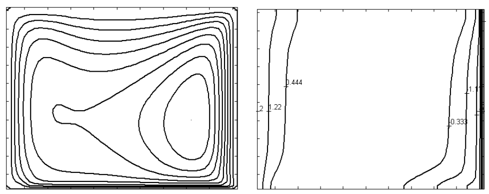

T_{min} = -5.0 and T_{max} = 2.0

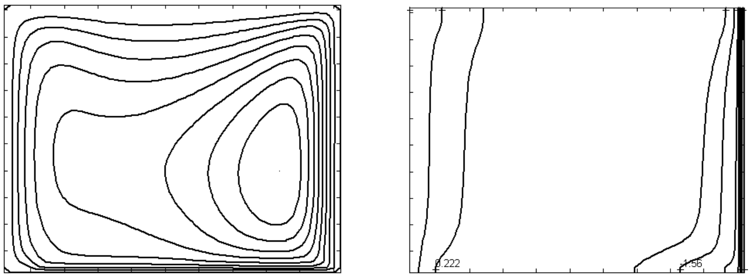

T_{min} = -6.0 and T_{max} = 2.0

Figure 3: Steady state streamlines and isotherms for Pr = 10

Nomenclatures

g = acceleration due to gravity
β = volume coefficient of thermal expansion
α = thermal conductivity
ρ = density
υ = kinematic viscosity
θ_h = hot wall temperature
θ_c = cold wall temperature
θ_0 = initial temperature
θ = temperature of fluid at any point
T = non-dimensional form of temperature
u,v = components of velocity along x and y directions respectively
U,V = non-dimensional forms of velocity components along X and Y directions respectively
ΔX,ΔY = grid spacing in the X and Y directions respectively
Δτ = time increment
ζ = dimensionless vorticity
ψ = dimensionless stream function
ω = relaxation parameter
Pr = Prandtl number
Gr = Grashof number
L = ratio of cavity height to its width

References

[1] Hamed, M.S and Folryan , J.M., The analysis of unsteady thermocapilary convection in a rectangular cavity, J. Fluid Mech. (1994).

[2] Kazmierczak, M and Chinoda, Z., Buoyancy driven flow in an enclosure with time periodic boundary condition, Int. J. Heat mass Transfer (1992), vol. 35, 1507-78.

[3] Schladow, S.G., Patterson, J.C and Street, R.L., Transient flow in a side-heated cavity at high Rayleigh number: a numerical study, J. Fluid Mech. (1989), vol. 200, 121-148.

[4] Vasseur, P and Robillard , L., Natural convection in a rectangular cavity with wall temperature decreasing at a uniform rate, (1982), vol. 16, 199-207.

[5] Wilkes, J.O and Churchill, S.W., The finite difference computation of natural convection in a rectangular enclosure, A.I. Ch. E.J., (1996), vol. 12, 161-166.

[6] Rudraiah, N., Venkatachalappa, M and Subbarayn, C.K., Combined surface tension and buoyancy driven convection in a rectangular open cavity in the presence of magnetic field Int. J. Non-linear mech. (1995) Vol. 35, 759-770.

[7] Kandaswamy, P., Sivasankaran, s., Bhavani Lakshmi, M. and Rama-swamy, R .S., Convection in a cavity with variable viscosity fluid, Indian J.pure appl. Math., (2005) Vol.36(11), 641-650

[8] John, D., and Anderson, J.R., "Computational Fluid Dynamics" McGraw-Hill International Editions (1995).

[9] Schlichting, H and Gerstew, K., "Boundary layer theory" Springer Publication, 8th Revised Edition (2001).

[10] Arora Domkudwar and Dom Kundwar, A.,"A course in heat and mass transfer" Dhanput Rai & co (2003).